

the radiation from the 330-kev resonance is suppressed strongly, showing that most of this radiation has energies lower than 5.6 Mev, in accordance with measurements of Carlson and Nelson.<sup>5</sup> The curve also shows that the radiation has a component of high-energy gamma rays, having a yield curve that rises smoothly through the whole region.<sup>6</sup> It is evident that a great part of the high-energy quanta observed by Carlson and Nelson belongs to the nonresonant part of curve IV.

Carlson and Nelson<sup>5</sup> have measured the gamma spectrum at a proton energy of 315 kev, and found that 8 percent go to the ground state, 20 percent to the first excited level, and the rest to still higher levels. The quanta going to the first excited level (gamma energy approximately 6.15 Mev) would contribute to curve IV, but because of the discriminator setting their efficiency would be greatly reduced compared to that

<sup>5</sup> R. R. Carlson and E. B. Nelson, *Phys. Rev.* **95**, 641 (1954).

<sup>6</sup> After this manuscript was written we extended the measurements of curve IV up to 550 kev with our new Van de Graaff machine. There is still a continuously increasing yield, and no indication of the resonance at 489 kev reported by Hunt.<sup>3</sup>

for quanta from transitions to the ground state. Pulses resulting from transitions to still higher levels would be completely suppressed.

Jacobs *et al.*<sup>7</sup> have found that the gamma radiation is isotropic. They used G.M. tubes, which means adding the effect of all different transitions. The distribution from one specific transition could still be anisotropic. We have measured the yield in one case at two different angles, relative to the direction of the proton beam. Curves I and IV are observed at 0°. With the same discriminator setting as in curve IV (5.6 Mev), we have observed the yield at 90° and, within the limits of error, have got the same ratio between the yields at 330 kev and at 500 kev. Therefore, if the angular distribution is not isotropic, at least it must be approximately the same for the two transitions contributing in this case.

This work was supported by the Royal Norwegian Council for Scientific and Industrial Research, as well as by a grant from "Fridtjof Nansens fond."

<sup>7</sup> Jacobs, Malmberg, and Wahl, *Phys. Rev.* **73**, 1130 (1948).

## Differential Elastic Scattering Cross Section for Neutrons on Nitrogen

J. L. FOWLER AND C. H. JOHNSON  
Oak Ridge National Laboratory, Oak Ridge, Tennessee  
(Received December 27, 1954)

Two independent methods were used to measure the angular distribution for elastic scattering of neutrons from nitrogen in the neutron energy range from 0.80 to 2.36 Mev. The scattered neutrons were counted directly in order to obtain the absolute differential cross section at four neutron energies. These curves provide information on the potential scattering for energies below 1.54 Mev. The second technique, which observed the recoil nitrogen nuclei, allowed a study of scattering at the resonances. In this manner parities were established for levels in N<sup>15</sup> as follows: The 1.120, 1.401, 1.595, and 2.25-Mev levels have odd parity; the 1.779-Mev level has even parity and a tentative assignment of even parity was made for the 1.350-Mev level. *J*-values associated with resonances at 1.12 and 2.25 Mev were each assigned to be 3/2 rather than the values favored in the literature.

### I. INTRODUCTION

IT has been recognized for a long time that differential elastic scattering neutron measurements yield valuable information about nuclear structure and resonance parameters. The differential scattering of 1-Mev neutrons from heavier elements<sup>1</sup> has been used as a test of the cloudy crystal ball model of the nucleus.<sup>2</sup> In this laboratory we have begun a systematic study of the resonance scattering of neutrons from light nuclei.<sup>3-5</sup> Nitrogen is an appropriate nucleus for such studies. There are a number of levels at relatively low energies<sup>6-9</sup>

so that one can accumulate information as to how the quantum properties vary from level to level. In general the levels have sufficient width ( $\sim 20$  kev) so that one can resolve them with standard techniques. The reaction cross sections of both (*n,p*) and (*n, $\alpha$* ) reactions are known<sup>10-12</sup> so that a comparatively complete theoretical analysis of the scattering process can be made. In the 2.6- to 4.2-Mev energy region measurements

<sup>1</sup> Hinchey, Stelson, and Preston, *Phys. Rev.* **86**, 483 (1952).

<sup>2</sup> Johnson, Willard, Bair, and Kington, Oak Ridge National Laboratory Physics Division Quarterly Report ORNL-1365, 1952 (unpublished), p. 1.

<sup>3</sup> Meier, Ricamo, Scherrer, and Zünti, *Helv. Phys. Acta* **26**, 451 (1953).

<sup>4</sup> C. H. Johnson and H. H. Barschall, *Phys. Rev.* **80**, 818 (1950).

<sup>5</sup> W. Bollmann and W. Zünti, *Helv. Phys. Acta* **24**, 517 (1951).

<sup>6</sup> Roseborough, McCue, Preston, and Goodman, *Phys. Rev.* **83**, 1133 (1951).

<sup>1</sup> M. Walt and H. H. Barschall, *Phys. Rev.* **93**, 1062 (1954).

<sup>2</sup> Feshbach, Porter, and Weisskopf, *Phys. Rev.* **90**, 166 (1953).

<sup>3</sup> Fowler, Johnson, and Risser, *Phys. Rev.* **91**, 441 (A) (1953).

<sup>4</sup> Willard, Bair, and Kington, *Phys. Rev.* **94**, 786 (A) (1954).

<sup>5</sup> C. H. Johnson and J. L. Fowler, *Phys. Rev.* **95**, 637 (A) (1954).

<sup>6</sup> Johnson, Petree, and Adair, *Phys. Rev.* **84**, 775 (1951).

have been reported<sup>13,14</sup> for the angular distribution of *d-d* neutrons elastically scattered from nitrogen. In the present work two independent methods were used to observe the scattering for neutron energies from 0.80 to 2.36 Mev. Section II describes the direct method of detecting the scattered neutrons in order to measure the absolute scattering cross section. Section III describes the more rapid but less accurate technique of detecting recoil nuclei. The last section discusses the results of both measurements.

## II. DETECTION OF SCATTERED NEUTRONS

Figure 1 shows the experimental arrangement for the neutron detection experiment, which is similar to that used by Walt and Barschall.<sup>1</sup> Briefly, neutrons from a source were scattered by a cylindrical sample and detected by a counter which was shielded from the direct neutron flux. Neutrons were produced in the  $T(p,n)He^3$  reaction. Analyzed protons from the 2.5 Mev Van de Graaff entered a tritium gas target of 25- to 50-kev stopping power through a 50 micro-inch nickel window. The neutron energy spread introduced by the foil was found to be 20 kev at 1.35 Mev by a simple transmission experiment which measured the experimental width of a known resonance<sup>7</sup> in the total cross section of nitrogen.

Scattering samples were formed from lithium azide ( $LiN_3$ ) prepared by the Analytical Chemistry Division at the Oak Ridge National Laboratory. According to a quantitative analysis, the sample was 14.14 percent by weight of Li and 83.94 percent by weight of nitrogen. For  $LiN_3$  these numbers are 14.17 and 85.83 so that a small error was introduced by assuming the sample to be pure. The  $LiN_3$  was transferred inside a dry box into a thin-walled (0.008 cm) brass can 2.8 cm in diameter and 11.4 cm long. This scatterer was placed at zero degrees to the proton beam with its axis perpendicular to the beam axis and 31.5 cm from the source. For background measurements an identical can was provided which contained the same amount of lithium as the original sample in the form of disks spaced along the axis of the can.

Neutrons scattered by the  $LiN_3$  were detected by a 1-atmosphere propane recoil counter having an active volume 9.5 cm long and 2.4 cm in diameter. At each neutron energy the propane counter bias was set to give an approximately flat response for neutrons scattered at all angles from nitrogen. Bias curves were obtained by comparison with a long counter<sup>15</sup> which was assumed to have a flat response over the small neutron energy range concerned. In order to measure the angular distribution of the neutrons scattered from nitrogen, the propane counter was placed with its center 13.7 cm from the center of the sample and was

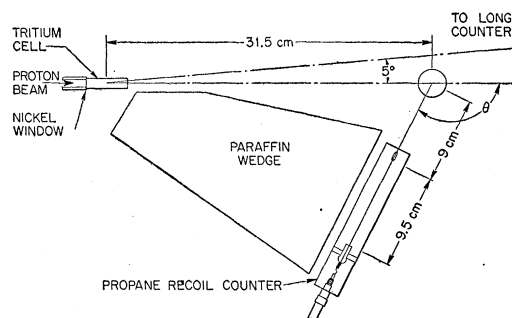


FIG. 1. Experimental arrangement for scattering of neutrons by lithium azide in order to measure the differential cross section for elastic scattering of neutrons by nitrogen.

rotated about the axis of the sample. At each angle a suitable paraffin slab shielded the counter from the direct flux. The sample, counter, and paraffin were each supported by wires; and the nearest massive supports were a grating floor 5.5 feet from the sample and a concrete floor 15 feet from the sample. Backgrounds, which varied from 50 percent for forward angles to 80 percent at backward angles, resulted primarily from air scattering.

The differential elastic scattering cross section was measured at nine angles by the following sequence of measurements: The paraffin and scatterer were removed, and the direct flux was determined by placing the propane counter at 5 degrees to the beam. This was the average angle of the scattering sample to the beam. For the measurement of the scattered flux the counter was moved to the desired angle,  $\theta$ , the paraffin was replaced, and alternate runs were made with the  $LiN_3$  and the Li samples in position. Finally, another direct flux measurement was made at five degrees to the beam before proceeding to the next angle. All measurements were monitored by the long counter at 5 degrees to the beam and 3.1 meters from the source. Distances to source, scatterer, and counter were recorded for each angle.

At an angle  $\theta$  the differential elastic scattering cross section is proportional to  $[C(\theta) - B(\theta)]/D$ , where  $C(\theta)$  is the number of counts with the scatterer in place,  $B(\theta)$  is the number of background counts with the lithium sample in place, and  $D$  is the number of direct counts. Each number is normalized by the long counter monitor. The calculation of the cross section requires the number of atoms in the sample; the distances between source, scatterer, and detector; and the aforementioned ratio. The counter efficiency cancels in the ratio. Since each component of the scattering geometry was finite, the following effects were considered:

(a) Effective distances were found by integration over the lengths of the source, scatterer, and detector. The active length of the detector was taken to be that of its counter wire and the effective center was found by observing the counting rate at several distances from the source.

<sup>13</sup> Baldinger, Huber, Ricamo, and Zünti, *Helv. Phys. Acta* **23**, 503 (1950).

<sup>14</sup> P. Huber and H. R. Striebel, *Helv. Phys. Acta* **27**, 157 (1954).

<sup>15</sup> A. O. Hanson and J. L. McKibben, *Phys. Rev.* **72**, 673 (1947).

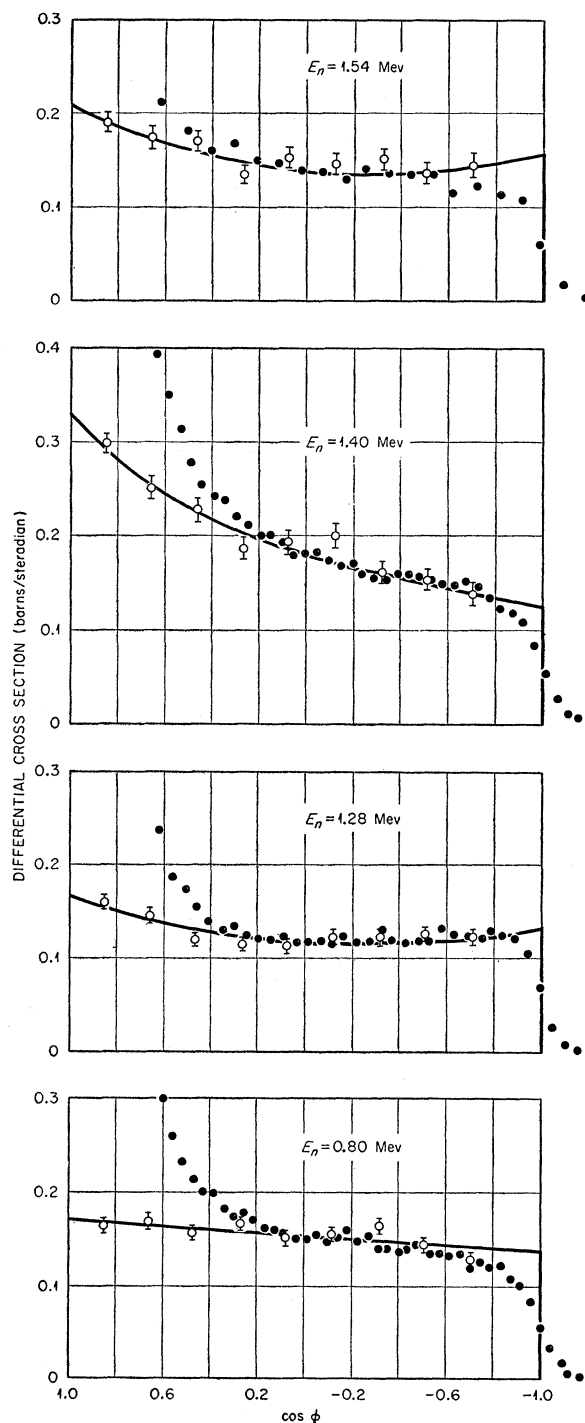


FIG. 2. Differential cross section in center-of-mass system for elastic scattering of neutrons by nitrogen in barns/steradian versus the cosine of the center-of-mass angle. Open circles show data from the neutron scattering experiment and solid points show the nitrogen recoil data. Curves are shown for three off-resonance points at 0.80, 1.28, and 1.54 Mev, and one resonance at 1.40 Mev.

(b) Direct neutrons were detected with the counter aimed at the target, whereas scattered neutrons entered

at an average angle of  $12^\circ$  to the counter axis. The ratio of sensitivities for the two directions was found experimentally to be 0.97. A correction was also made for a slight variation of counter efficiency with the scattered neutron energy.

(c) The measured cross section is an average over the angular resolution of the counting geometry and is plotted at an average angle which is larger than the angle between the counter and proton beam axis. The full width at half-maximum of the angular resolution function stated in terms of the cosine of the scattering angle was less than 0.2. In the analysis of the results the correction for angular resolution was small.

(d) The sample partially shields itself from the incident flux. The ratio of the average flux within the sample to the incident flux was found from known total cross sections<sup>7</sup> to range from 0.91 to 0.94.

(e) Since the diameter of the samples was about one-fifth of a mean free path for scattering, some of the neutrons were scattered more than once. To correct for this the approximate angular distribution was first determined with the above effects included and then a multiple scattering correction was made following Walt and Barschall.<sup>1</sup> Off-resonance the correction was very small, but the correction for the 1401-keV resonance curve was as large as 6 percent. No correction was made for multiple scattering by the lithium.

Figure 2 shows the differential elastic scattering cross section versus the center-of-mass scattering angle for neutron energies of 0.80, 1.28, 1.40, and 1.54 Mev. The open circles are the data from the experiment described above; the solid points are discussed in the following section. The vertical bars on the open circles indicate the standard statistical deviation of the data points. Average curves have been drawn through the points and an integration under each curve yields a cross section which agrees within the statistical uncertainty with the elastic part<sup>7,10</sup> of the total cross section. This measures the accuracy of the approximations which were used. In particular the effect of the impurity in the scatterer has been neglected. If this impurity were  $H_2O$  or a hydroxide, then the distributions, particularly at lower neutron energies, would show strong scattering at the two most forward angles. At those angles the propane counter was not biased against neutrons scattered from hydrogen. The absence of a forward peak in the 0.8-Mev curve indicates the impurity contains little hydrogen. Other impurities would cause a negligible distortion of the curves.

### III. DETECTION OF RECOIL NITROGEN NUCLEI

In the absence of inelastic scattering, the angular distributions of elastic scattering of neutrons can be deduced from the energy distribution of the recoil nuclei.<sup>16,17</sup> The energy of the recoil nucleus is propor-

<sup>16</sup> Baldinger, Huber, and Staub, *Helv. Phys. Acta* **11**, 245 (1938).

<sup>17</sup> H. H. Barschall and M. H. Kanner, *Phys. Rev.* **58**, 590 (1940).

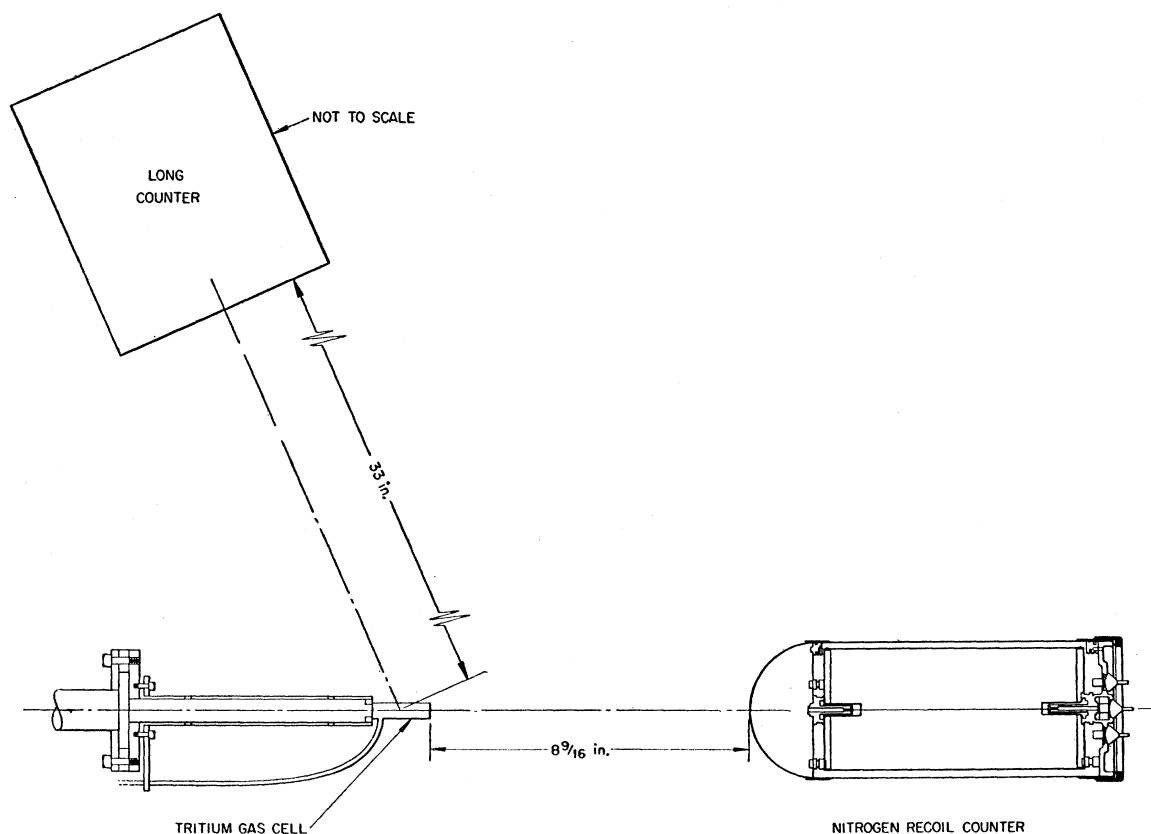


FIG. 3. Experimental arrangement for observing the energy distribution of nitrogen recoils caused by elastic scattering of neutrons by nitrogen.

tional to  $(1 - \cos\phi)$ , where  $\phi$  is the neutron scattering angle in the center-of-mass system. In this system also the number of recoils in energy interval  $\Delta E$  is proportional to the differential scattering cross section times the interval  $\Delta(\cos\phi)$ . Since energy pulse-height analysis is a more rapid technique than the detection of scattered neutrons, we have used the nuclear recoil technique to investigate the intermediate-width resonances in nitrogen with better neutron energy resolution than was used in the neutron detection experiment.

Recoils were detected with a nitrogen-filled proportional counter, Fig. 3, with a cylindrical active volume 7.62 cm in diameter and 12.7 cm long. The length<sup>18</sup> was defined by field tubes<sup>18</sup> which eliminated end effects resulting from nonuniform fields. The counter wire was separated from the field tube voltage by grounded shield tubes. Pulses from the counter were amplified by ORNL A-1 preamplifiers and amplifiers<sup>19</sup> with a band pass of 0.5 Mc. During the earlier stages of this experiment pulses were analyzed with an ORNL single-channel analyzer,<sup>20,21</sup> and later on a 20-channel

pulse-height selector was used.<sup>22</sup> The relative voltage of the cathode and field tube were adjusted to give best energy resolution. With the counter filled with a gas mixture of 2 atmos A and  $\frac{1}{2}$  atmos  $N_2$ , the counter system resolved the 630-kev peak from the  $N^{14}(n,p)C^{14}$  reaction produced by thermal neutrons with a full width at half-maximum of 5 percent.

Figure 3 shows the experimental arrangement for the recoil experiment. Neutrons were produced by the  $T(p,n)He^3$  reaction as discussed in Sec. II except that protons were accelerated by both the 5.5-Mev and 2.5-Mev Van de Graaffs. At a few neutron energies, higher resolution was obtained by replacing the gas target with zirconium-tritide. The long counter monitored the neutron flux. The recoil counter was filled to about  $\frac{1}{4}$  atmos  $N_2$  and placed with its axis at  $0^\circ$  to the proton beam. The energy scale for neutrons entering the counter was established by using the recoil counter with low bias settings as a detector to locate known resonances in the total cross section of nitrogen.<sup>6-9</sup> Experimental widths of the observed resonances corrected for the known natural widths gave the neutron energy resolution. This energy resolution varied from 10- to 40-kev

<sup>18</sup> A. C. Cockcroft and S. C. Curran, *Rev. Sci. Instr.* **22**, 37 (1951).

<sup>19</sup> W. Jordan and P. R. Bell, *Rev. Sci. Instr.* **18**, 703 (1947).

<sup>20</sup> Francis, Bell, and Gundlach, *Rev. Sci. Instr.* **22**, 133 (1951).

<sup>21</sup> J. E. Francis and P. R. Bell, Oak Ridge National Laboratory Report ORNL-1470 (unpublished).

<sup>22</sup> Kelley, Bell, and Goss, Oak Ridge National Laboratory Physics Division Quarterly Progress Report ORNL-1278, 1951 (unpublished).

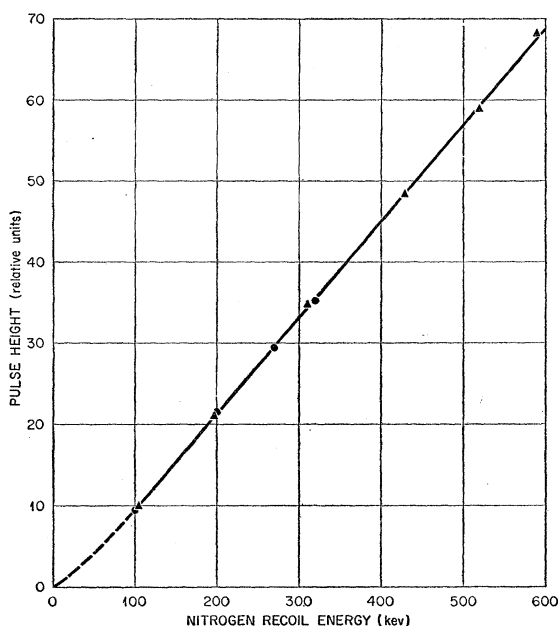


FIG. 4. Linearity check of pulse height *versus* energy in the nitrogen counter. The pulse height corresponding to the mean of the upper edge of several pulse height distributions for nitrogen recoils is plotted against the maximum recoil energy.

full width at half-maximum, with most of the data taken with 20-kev resolution.

For purposes of comparison, pulse-height distributions were obtained with the recoil counter at the same neutron energies and energy resolutions as those used for the direct measurements of the last section. Since the nitrogen-recoil energy scale is a linear function of  $\cos\phi$ , one can adjust the upper edge of the pulse-height distributions to the line  $\cos\phi = -1.0$  and thereby make a direct comparison with the differential cross sections. In Fig. 2 the solid points are the nitrogen-recoil data, and open points are scattered-neutron data. A rough measurement showed that the total number of pulses was about equal to the number of recoils expected from the source strength and counting geometry; however, in Fig. 2 the recoil data have been arbitrarily normalized for convenient comparison.

In the recoil pulse-height distributions of Fig. 2 and of other figures to be presented, the energy scale or equivalent  $(1 - \cos\phi)$  scale has been corrected for a slight nonlinear pulse-height variation with energy. The correction was found from Fig. 4 which shows the pulse height corresponding to the mean of the upper edge of a number of distributions *versus* the maximum recoil energy (0.249 times the incident neutron energy).

A number of tests were made to check the reproducibility of pulse-height distributions for 0.8-Mev neutrons. The nitrogen pressure in the counter was changed by a factor of three. The counter voltage and consequently the gas multiplication was varied over a considerable range. The tritium neutron source was

altered; Al was substituted for Ni as the tritium cell window, and the experiment was performed with a zirconium-tritide target. While there was some fluctuation of the curves for  $\cos\phi > 0.8$ , the distributions otherwise were essentially the same. The relative distributions obtained at other energies were reproducible within the statistical errors of the measurements which are indicated by the fluctuations of the solid points in Fig. 2 from a smooth curve.

The number of pulses resulting from background neutrons was determined by substituting helium for tritium in the gas cell, and was found to be negligible for the upper  $\frac{3}{4}$  of the energy distributions. At 1.40 Mev it was necessary to subtract a background resulting from the  $N^{14}(n,p)C^{14}$  reaction which is not a negligible part of the total cross section at this resonance. Since the protons are not stopped in the counter gas, they give rise to a continuum rather than a discrete pulse group. An approximate correction was made with the assumption that the  $(n,p)$  pulses are uniformly distributed from zero to a pulse height corresponding to 540 kev, the maximum energy loss in the counter. No correction is required for the  $(n,\alpha)$  reaction since most  $\alpha$  particles stop in the counter gas and give a discrete group at larger pulse height than the maximum recoil pulse.

Figure 2 indicates that except for the straggling at the upper edge due to the energy resolution of the counter, the nitrogen recoil distributions agree approximately with the differential cross-section data in the region  $0 < \cos\phi < -1$  but begin to deviate at  $\cos\phi > 0.1$ . A small part of this disagreement for  $\cos\phi > 0.1$  is due to the nonlinear dependence of recoil pulse height on neutron energy. The comparison presented in Fig. 2 enables one to plot relative correction curves for the off-resonance recoil data as a function of energy for the angular region  $0.5 > \cos\phi > 0$ .

For the study of a resonance by the recoil technique, a series of distribution curves were taken in a continuous series of runs: a distribution between the resonance and the resonance below it; a distribution at the peak of the resonance and in some cases on the sides of the peak; and a distribution between the resonance and the resonance above. The extrapolated relative corrections were applied to the resonance data up to 1.7 Mev; beyond that the correction was negligible.

In Figs. 5, 6, and 7 the solid circles show the nitrogen recoil data which have been normalized for comparison with the theoretical differential cross-section curves discussed in the next section. The neutron total cross section taken from the literature<sup>7-9</sup> is plotted on the right-hand side of the figures. The arrows indicate the neutron energy at which the differential cross section and angular distribution measurements were made. The bars at the end of the arrows give the full energy spread at half-maximum for the neutrons entering the counter.

IV. DISCUSSION OF RESULTS

The method of analysis of Blatt and Biedenharn<sup>28</sup> allows one to calculate theoretical neutron differential elastic scattering cross sections at resonances providing one knows the phase shifts for potential scattering and the quantum parameters of the resonances. The off-resonance scattering cross sections obtained from the neutron detection experiment were used to deduce the potential phase shifts. A Legendre polynomial fit was made to the experimental curves through the cross-

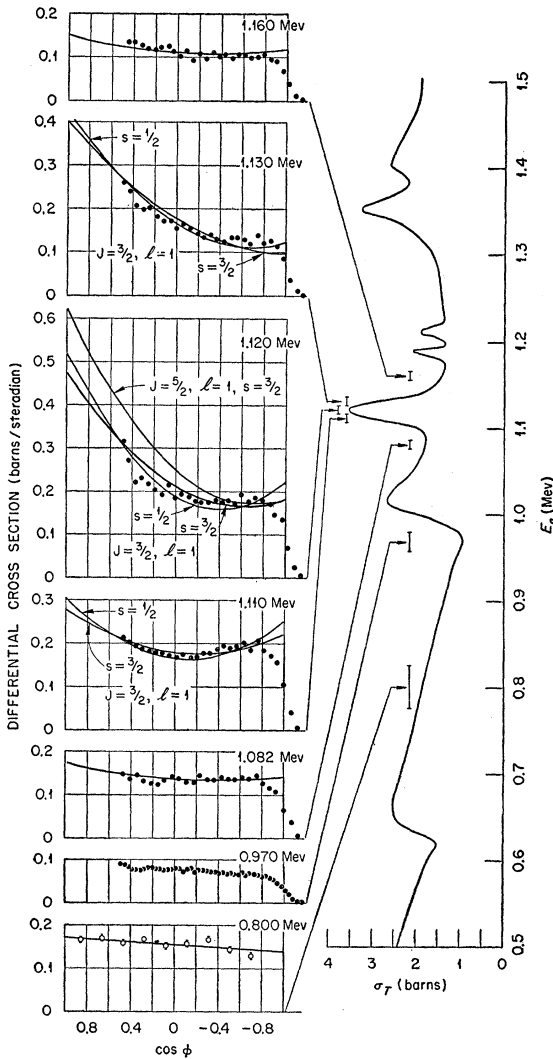


FIG. 5. Differential cross section in center-of-mass system for scattering of neutrons by nitrogen in barns/steradian versus the center-of-mass scattering angle. Curves are given for several energies from 0.80 to 1.16 Mev. The total cross section of nitrogen is plotted at the right, and connecting arrows indicate the neutron energy for each distribution. Open circles are neutron scattering data and closed circles are nitrogen recoil data. Theoretical curves are given; and near the resonance they are labeled with total angular momentum ( $J$ ), orbital angular momentum ( $l$ ), and channel spin ( $s$ ).

<sup>28</sup> J. M. Blatt and L. C. Biedenharn, *Revs. Modern Phys.* **24**, 258 (1952).

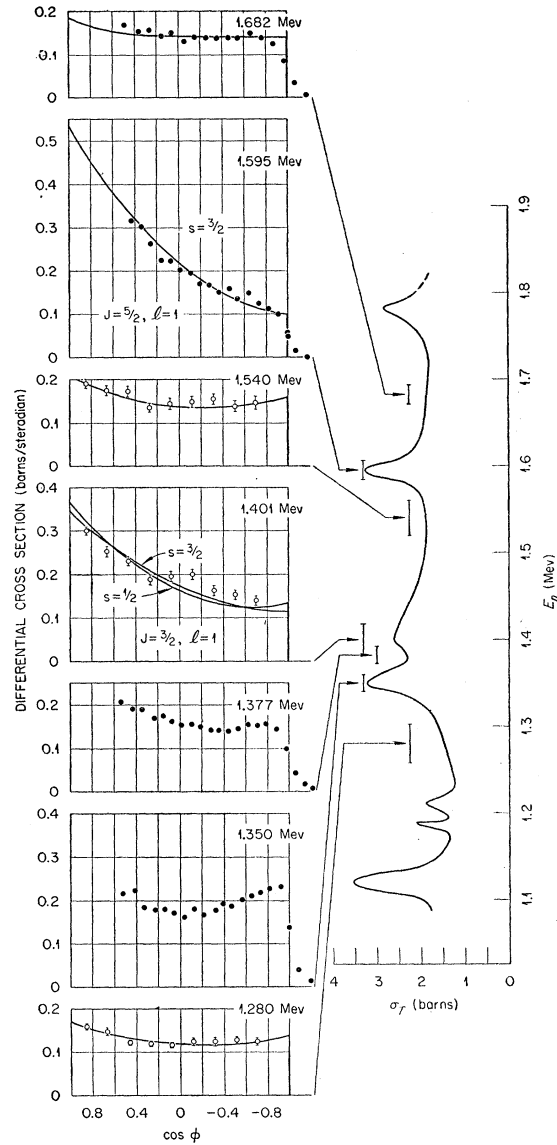


FIG. 6. An extension up to 1.682 Mev of the differential cross-section curves described in Fig. 5.

section data, and the phase shifts were calculated from the coefficients of the polynomials. Figure 8 shows a plot of the empirical potential phase shifts for  $s$ - and  $p$ -waves versus laboratory neutron energy. Below 800 kev the potential scattering was assumed to be all  $s$ -wave, so that the phase shift is found from the total cross section by the relation:  $\sigma_t = 4\pi\lambda^2 \sin^2\eta_0$ , where  $\lambda$  is wavelength of relative motion divided by  $2\pi$ , and  $\eta_0$  is the  $s$ -wave phase shift. For the higher energy points, the analysis indicated a slight amount of  $d$ -wave phase shift  $< 3^\circ$ ; however, the presence of tails of near resonances and inaccuracies in the experimental distributions made the use of  $d$ -wave phase shift in the calculation unjustifiable. The dashed curves in Fig. 8 give the  $s$  and  $p$  phase shifts expected from the hard-sphere

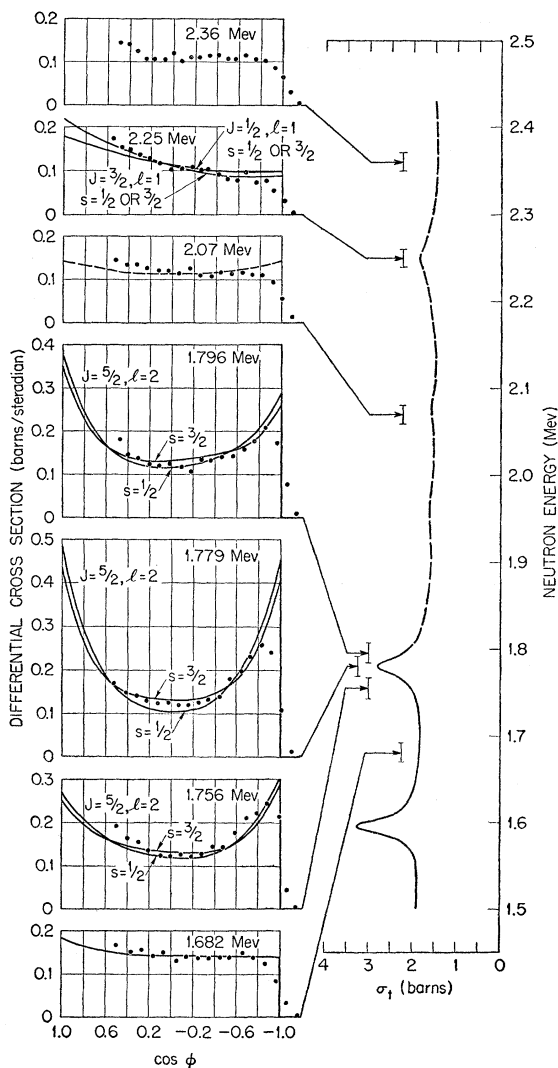


FIG. 7. An extension from 1.682 to 2.36 Mev of the differential cross-section curves described in Fig. 5.

scattering. The behavior of the experimental  $\eta_0$  is probably connected with shape resonance discussed by Feshbach, Porter, and Weisskopf,<sup>2</sup> and Adair.<sup>24</sup> In Figs. 5, 6, and 7 the experimental phase shifts from Fig. 8 have been used to describe the off-resonance distributions obtained from the recoil data.

The above calculation includes the assumption that the phase shifts for the two channels are equal. The approximate equality of coherent and incoherent bound nuclei scattering at thermal energies<sup>25,26</sup> and the depth of the interference dip before the 639-keV ( $J=1/2$ )  $s$ -resonance support this assumption. The dip before the 998-keV ( $J=3/2$ )  $s$ -resonance is not enough to be explained on the basis of equal phase shifts for both

<sup>24</sup> R. K. Adair, Phys. Rev. **94**, 737 (1954).

<sup>25</sup> C. G. Shull and E. O. Wollan, Phys. Rev. **81**, 527 (1951).

<sup>26</sup> A. W. McReynolds and G. W. Johnson, Phys. Rev. **82**, 344(A) (1951).

channel spin states; nevertheless, the magnitude of the total cross section and the analysis of the angular distribution at about 1.65 Mev indicate that both channel spin phase shifts are approximately  $90^\circ$  at this higher energy.

It will be seen from that which follows that for the case of elastic scattering of neutrons from nitrogen a qualitative analysis of the resonance angular distributions is simple, since the potential phase shift is negative and predominantly  $s$ -wave. At resonance energies for  $J=3/2$  or  $5/2$ ,  $p$ -wave neutrons will show forward scattering, and  $d$ -wave neutrons will show both forward and backward scattering nearly symmetrical about  $90^\circ$ .

In Figs. 5, 6, and 7, curves are presented which give the quantitative analysis of the angular distributions at or near resonances. Below 1.54 Mev the potential scattering is assumed to be all  $s$ -wave, but above this energy  $p$ -wave is also included. In calculating the interference between the potential and resonance scattering for the 1.120, 1.401, 1.595, and 1.779-Mev levels, the  $J$ -values and ratio of neutron widths to total widths were taken from the paper of Hinchey, Stelson, and Preston,<sup>7</sup> who obtained these quantities from their total cross section measurements and from the  $(n,p)$  and  $(n,\alpha)$  cross sections.<sup>10,12</sup> The theoretical curves shown as lines through the resonance scattering data have been corrected for the energy spread of the source neutrons. The distribution of source neutrons was taken to be Gaussian with a full width at half-maximum given by the bars at the ends of the arrows which indicate the energy in the figures. The total angular momentum ( $J$ ) of the level as well as the orbital angular momentum ( $l$ ) of the neutrons and the channel spin ( $s$ ) are indicated on the curves. The slight energy dependence of the level width and level shift has been neglected.

It has been assumed throughout the discussion that each resonance is isolated from the others. On this

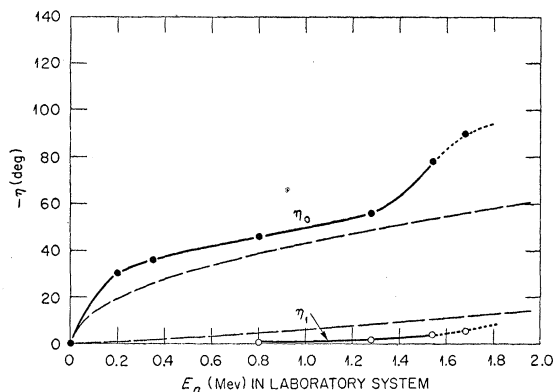


FIG. 8. Phase shifts for  $s$ - and  $p$ -wave potential scattering required to fit the off-resonance differential cross section for scattering neutrons by nitrogen. The solid curves are derived from the total cross sections and the neutron scattering data. The dotted parts of the curves are based on the total cross sections and the nitrogen recoil data. The dashed curves are phase shifts calculated for neutrons scattered from a hard sphere of radius  $3.7 \times 10^{-13}$  cm.

basis an analysis could not be made for the 1.35-Mev resonance which is near the broad 1.40-Mev resonance. It was assumed, however, that this narrow peak did not disturb the broad 1.40-Mev resonance.\* The 1.35-Mev resonance distribution suggests *d*-wave interaction.

An integration, times  $2\pi$ , under the theoretical curves for either channel spin yields the total elastic scattering cross section (to be observed with this energy resolution). This follows because the potential phase shifts were chosen to fit the absolute off-resonance cross section and the *J*-value has been assigned from the observed total cross section at resonance.

In the case of the 1.120-Mev level, the differential cross section is calculated for both  $J=3/2$  and  $5/2$ . Work on total cross section did not give a definite decision between these cases.<sup>7</sup> As is seen from Fig. 5 the angular distribution data favor  $J=3/2$ . Furthermore, with  $J=3/2$  and  $\Gamma_n/\Gamma=1$ ,<sup>7</sup> the theoretical resonance part of the total cross section is 1.78 barns which is consistent with an experimental estimate of the resonance part of the total cross section of about 1.9 barns (Fig. 4, reference 7<sup>27</sup>).

An analysis of the 2.25-Mev resonance is not as straightforward as that for the lower energy resonances. Johnson *et al.*<sup>8</sup> and Meier *et al.*<sup>9</sup> each observe a 0.38-barn peak which, corrected for the energy resolution, is a 0.41-barn resonance in the total cross section. The following discussion makes the assumption, which is not wholly justified, that this is an isolated resonance. The potential scattering phase shifts extrapolated in Fig. 8 to 2.25 Mev and adjusted to give the correct off-resonance cross section were taken to be  $\eta_0 = -100^\circ$  and  $\eta_1 = -10^\circ$ . This rough extrapolation and the neglect of *d*-wave phase shift are considered sufficiently accurate to use in assigning parity to the 2.25-Mev resonance. In Fig. 7, the dashed distribution at the off-resonance 2.07-Mev energy results from these phase shifts. The adjustment of *s*- and *p*-wave phase shifts and the addition of a *d*-wave contribution to force a better fit are not justified without a knowledge of the forward scattering. It is clear, nevertheless, that the potential scattering is predominantly *s*-wave and that the forward scattering at the 2.25-Mev resonance results

\* Note added in proof.—A qualitative investigation of the effect of the interference of the 1.35-Mev level on the angular distribution of the 1.40-Mev level shows the parity assignment based on the aforementioned analysis is not altered [A. E. Glassgold, Oak Ridge National Laboratory (private communication)].

<sup>27</sup>In reference 7 the  $\lambda_n^2$  were incorrectly transformed to the center-of-mass system; the value should be increased by the factor 15/14. P. H. Stelson (private communication).

TABLE I. *J*-values and parities for  $N^{15}$  levels which give rise to resonances in neutron scattering from nitrogen.

Neutron energy in Mev (laboratory system)	<i>J</i> -value	Parity
1.120	3/2	<i>o</i>
1.350	...	<i>e<sup>a</sup></i>
1.401	3/2	<i>o</i>
1.595	5/2	<i>o</i>
1.779	5/2	<i>e</i>
2.25	3/2	<i>o</i>

<sup>a</sup> Tentative assignment.

from *p*-wave neutrons. For *p*-wave neutrons there will be only a small interference dip so that the magnitude of the peak in total cross section is equal to approximately  $4\pi\lambda^2[(2J+1)/6](\Gamma_n/\Gamma)$ . Thus, taking into account the interference dip, one finds  $\Gamma_n/\Gamma=0.97$  or  $0.48$  for  $J=1/2$  or  $3/2$ , respectively. The choice between *J* values depends on the observed (*n,p*) and (*n, $\alpha$* ) cross sections. By substitution of these values in the expression  $4\pi\lambda^2[(2J+1)/6][\Gamma_n(\Gamma-\Gamma_n)/\Gamma^2]$ , one finds a reaction cross section of 0.01 barn for  $J=1/2$ , and 0.22 barn for  $J=3/2$ . Bollman and Züntli<sup>11</sup> observed a resonance [*(n,p)*+*(n, $\alpha$ )*] cross section of  $0.12\pm 0.04$  barn, which, corrected for energy resolution, agrees approximately with 0.22 barn. These considerations lead to an assignment of  $J=3/2$  in disagreement with the value,  $J=1/2$ , of Meier *et al.*

In Fig. 7 the theoretical angular distribution is presented at 2.25 Mev for  $J=3/2$ ,  $l=1$ ,  $\Gamma_n/\Gamma=0.48$ . Nearly identical curves are obtained for the two channel spins. A curve is also shown for  $J=1/2$  using the value,  $\Gamma_n/\Gamma=0.63$ , which had been assumed by Meier *et al.* The angular distribution favors  $J=3/2$ .

Table I gives a summary of the *J*-values and parities which give the best fit to the angular distribution data presented here. The tentative assignment for the 1.35-Mev resonance is based on a similarity of the angular distribution to that at 1.779 Mev. In assigning these parities to the excited states of  $N^{15}$ , the parity of  $N^{14}$  is taken to be even.

## V. ACKNOWLEDGMENTS

The authors are indebted to D. E. Lavallo for the preparation of the lithium azide and to R. E. Zedler for aid in the design and construction of the nitrogen recoil counter. We are particularly indebted to Dr. J. R. Risser for his active participation in the early stages of this experiment.<sup>3</sup>